CONF-890585--3

UCRL-PREPRINT 99492

The Effect of Gradients in HMX/TNT Content and Porosity on Shaped Charge Jet Characteristics

Michael J. Murphy

This paper was prepared for submittal to
the 11th International Symposium on Ballistics
Brussels, Belgium, May 09-11, 1989

February 9, 1989

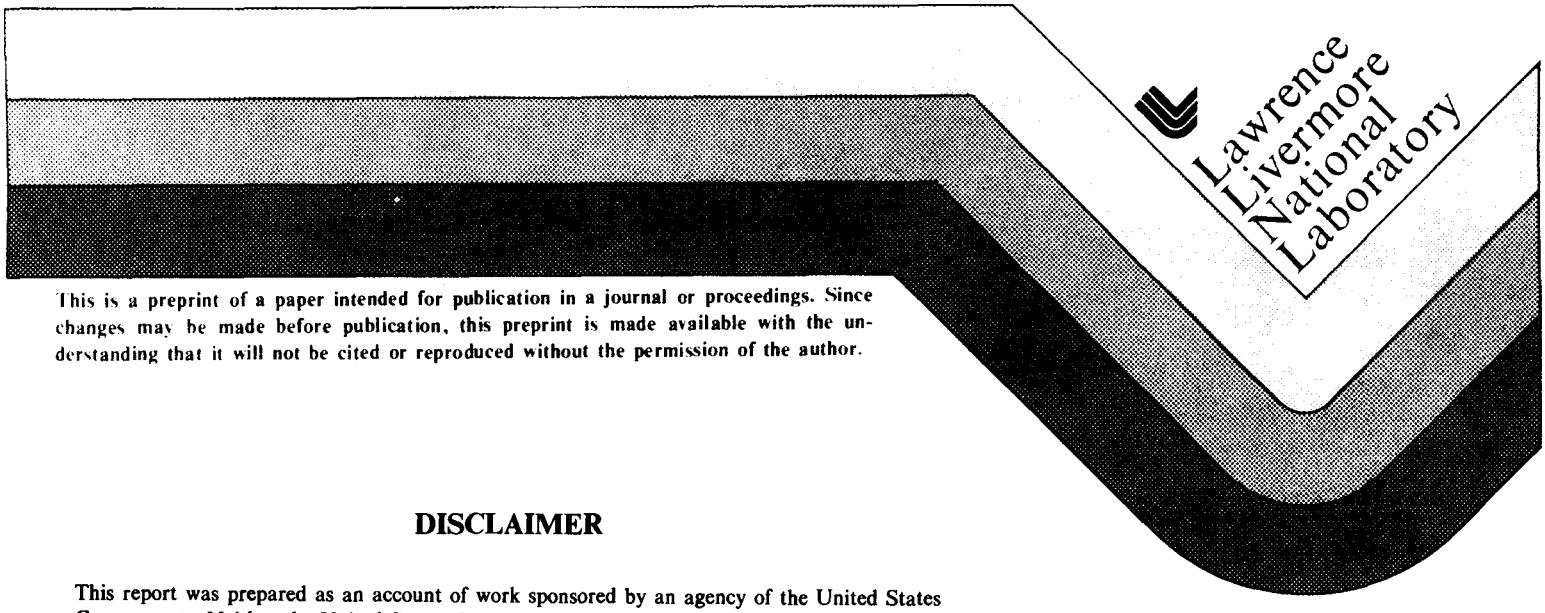

DISCLAIMER

UCRL--99492

DE89 008043

The Effect of Gradients in HMX/TNT Content and Porosity on Shaped Charge Jet Characteristics *

Michael J. Murphy
University of California
Lawrence Livermore National Laboratory
P. O. Box 808, Livermore, California 94550

Variations in shaped charge jet characteristics due to density gradients in melt cast Octol high explosive is studied. A family of JWL equations of state for Octol at various HMX/TNT contents and porosity is presented. 2-D finite element computations are evaluated to determine the effects of both axial and circumferential density gradients on jet characteristics.

1.0 OVERVIEW

Sedimentation melt cast explosives are widely used in the loading of charges for research and development as well as for production loading of shaped charges and other explosively driven systems. In particular, Octol is the preferred sedimentation melt cast explosive for development work due to its flexibility of fabrication and high energy density. High energy, precision PBX explosives such as LX-14 are certainly more desirable, however, cost, availability, tooling and machining factors result in the continued use of Octol. Everyone who uses Octol realizes that there is a potential drawback in the HMX/TNT sedimentation melt cast process which results in density gradients in the high explosive. The objective of this paper is to quantify the effects of the density gradients in Octol loaded charge as a function of HMX/TNT content and porosity.

* Work performed under the auspices of the U.S. Department of Energy by the Lawrence Livermore National Laboratory under contract No. W-7405-ENG-48.

2.0 DENSITY GRADIENT IN TYPICAL CHARGE

The density gradients that exist in sedimentation melt cast Octol high explosive shaped charges are due to variations in both HMX/TNT content and porosity of the explosive fill. Variation in the HMX/TNT content is due to a non-uniform distribution of the HMX particles within the TNT. This is the result of keeping the Octol at a temperature above the melt temperature of TNT and below the melt temperature of HMX. The molten TNT and solid HMX particles combined with the higher density of HMX over TNT produces sedimentation of the HMX to the lower portion of the charge. The resulting density gradient can be large or small depending on the loading procedure that is used. Porosity in the explosive is due to air entrapped in the Octol during the pouring and cooling process. Neither of these effects can be accurately detected by radiographs and a density measurement of a core sample only defines the density, it does not define the HMX/TNT content and corresponding porosity that result in the specific density measured.

The density and HMX/TNT composition of a typical shaped charge is shown in Figure 1 [1]. Determination of both the density and HMX/TNT content allows one to ascertain the level of porosity in the charge. The table on the right in Figure 1 gives the density and HMX/TNT content measured in the regions shown. A plot of Octol density as a function of HMX/TNT content and porosity is shown in Figure 2. Data points for the typical charge indicate a nominal level of porosity of 0.8%. Also shown on this plot is 78/22 Octol at 1.821 g/cc. This data point represents the HE material used for the Octol JWL EOS published in the LLNL Explosives Handbook [2]. This figure shows graphically that just measuring density does not specificaly define the material unless one assumes a particular level of porosity or HMX/TNT content.

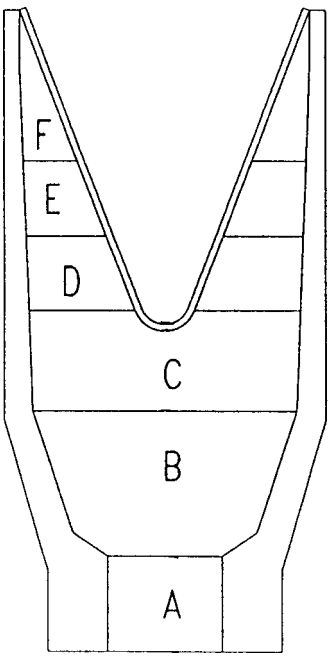

Region	Density	HMX/TNT
A	1.800	65/35
B	1.810	70/30
C	1.815	72/28
D	1.822	75/25
E	1.832	79/21
F	1.850	85/15

Figure 1. Density and HMX/TNT content of typical charge.

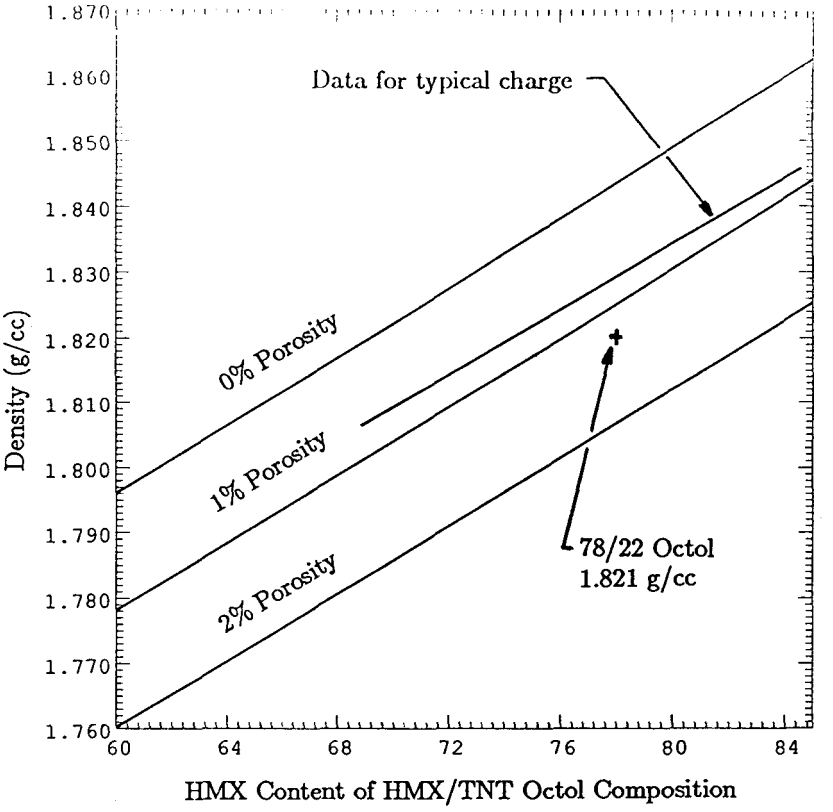

Figure 2. Octol density as a function of HMX/TNT content and porosity.

3.0 EXPLOSIVE PROPERTIES

The detonation velocity, c-j pressure , and energy of the various Octol compositions were calculated with the thermodynamic hydrodynamic code TIGER [3] using the BKW form of the equation of state, which predicts the detonation properties of condensed explosives. Normalization of TIGER with the BKW EOS was first accomplished by adjusting the BKW input variables until the detonation parameters for 78/22 Octol at 1.821 g/cc matched the values published for the JWL equation of state for explosive products. The tiger calculations of detonation velocity and c-j pressure are plotted as a function of HMX/TNT content and porosity in Figures 3 & 4. The relative energies at a volume expansion of 3.0 are plotted in Figure 5. This energy is referenced to 78/22 Octol at 1.821 g/cc.

A summary plot showing how both density and energy varry with HMX/TNT content and porosity is presented in Figure 6. The figure shows the explosive density as a function of HMX/TNT content at three levels of porosity as was presented in Figure 2. The eight crossing lines are curves of constant relative energy referenced to the 78/22 Octol at 1.821 g/cc. Assuming porosity in a typical charge to be fairly constant, Figure 6 shows that every 0.01 g/cc change in density results in about a 2.2% change in explosive energy. This figure also shows that at constant density, a 2% change in porosity and corresponding change in HMX/TNT content results in a 5% change in explosive energy.

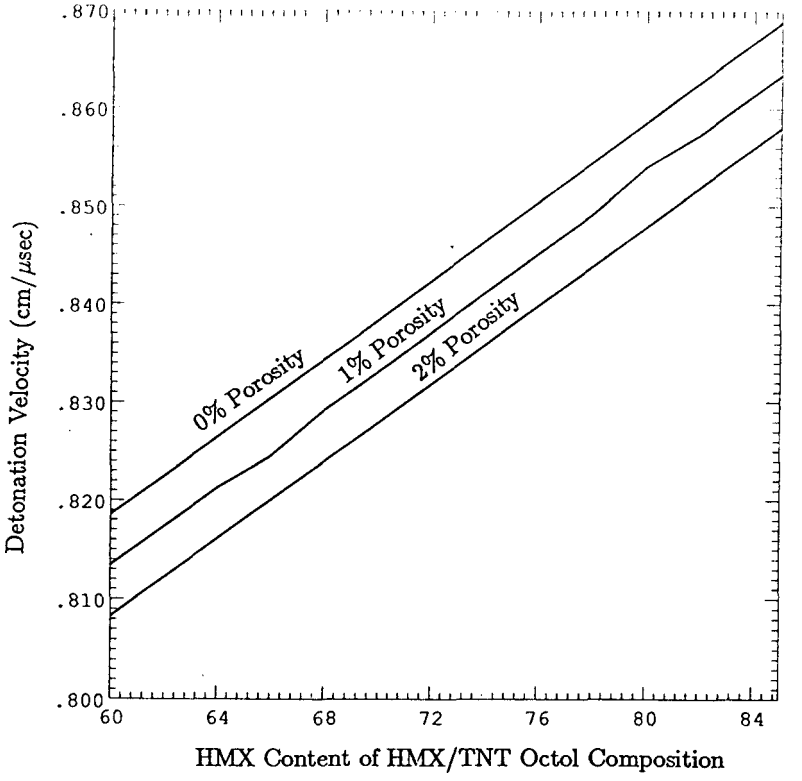

Figure 3. Detonation velocity as a function of HMX/TNT content and porosity.

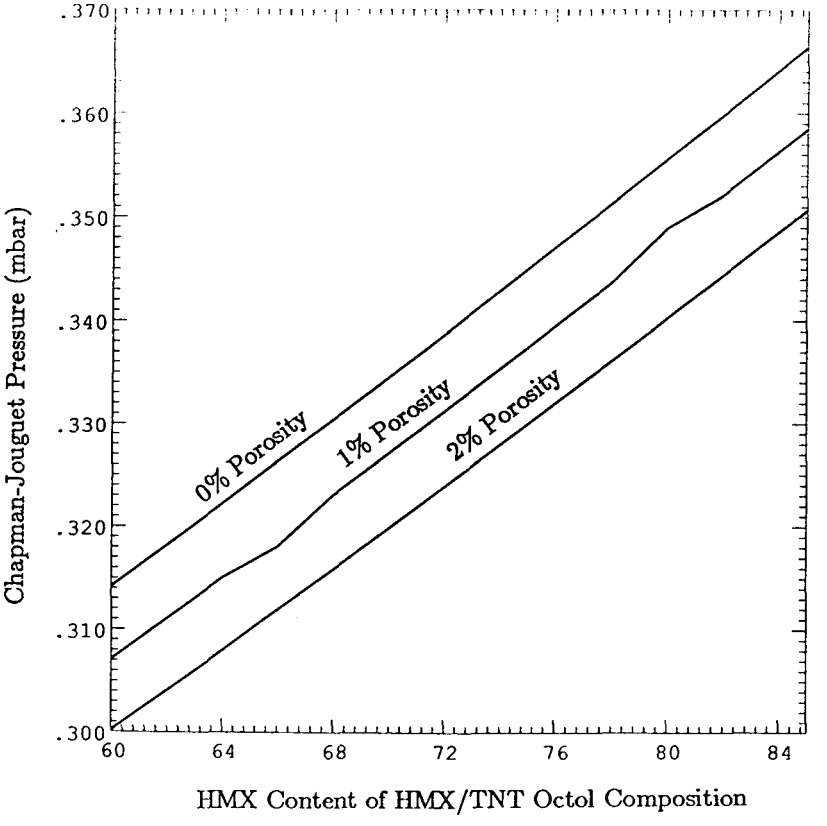

Figure 4. C-J pressure as a function of HMX/TNT content and porosity.

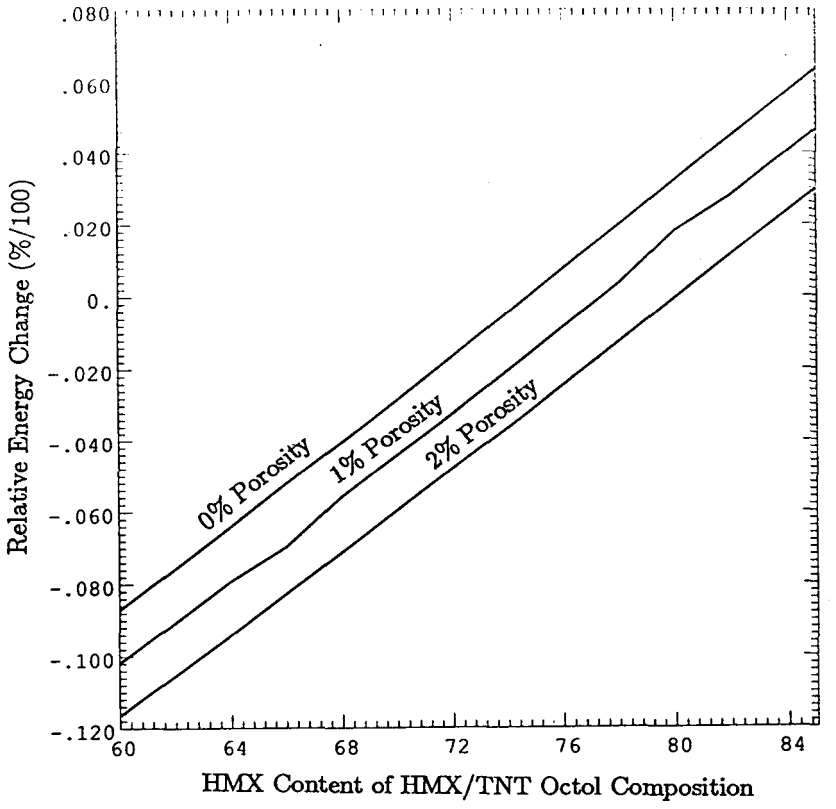

Figure 5. Relative energy change, referenced to 78/22 Octol at 1.821 g/cc as a function of HMX/TNT content and porosity.

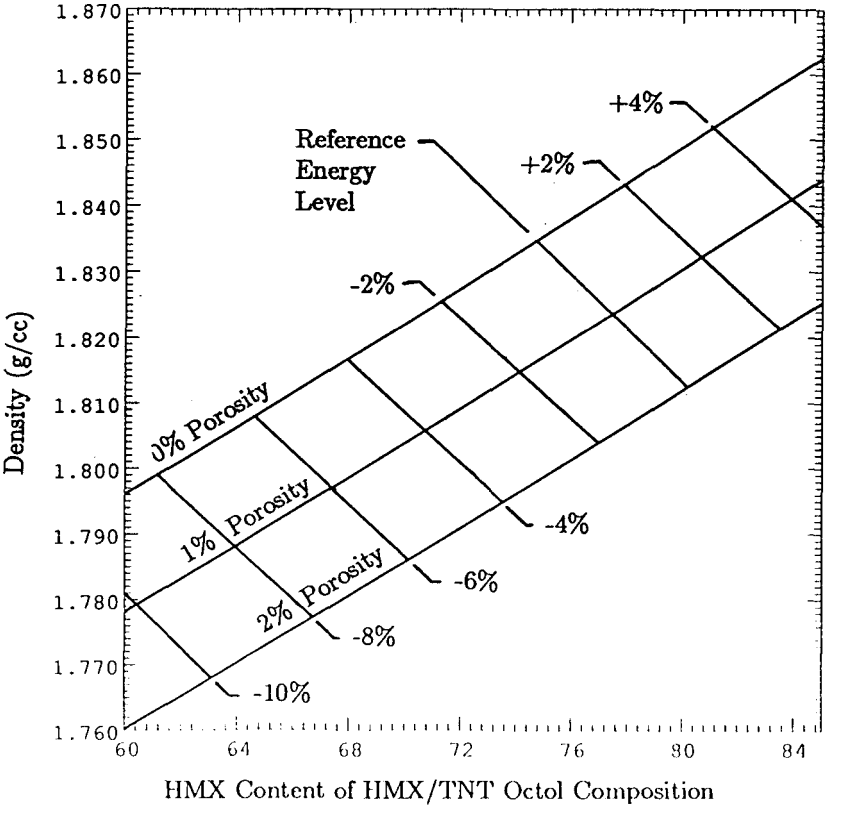

Figure 6. Description of density and energy variation as a function of HMX/TNT content and porosity.

4.0 JWL EQUATION OF STATE

The JWL EOS defines the pressure in the HE expansion products as;

$$P = A(1 - \omega/R_1V)e^{-R_1V} + B(1 - \omega/R_2V)e^{-R_2V} + \omega E/V$$

where A, B, R_1, R_2, and ω are empirical constants [4]. Several JWL equations of state were developed for the various Octol compositions using the approach described in Reference 4. The linear coefficients A and B are determined from the explosive properties D, P_cj, E_0, and ρ and the somewhat arbitrary yet appropriate selection of the non-linear coefficients R_1, R_2, and ω. The EOS is then used in a hydrodynamic calculation and compared with experiment.

The JWL EOS parameters for 78/22 Octol at 1.821 g/cc were used as a reference for developing EOS's for the various Octol compositions considered in this paper. The new EOS's were developed by keeping R_1, R_2, and ω constant, and specifying the appropriate detonation velocity, c-j pressure, and density as defined by the TIGER calculations. Determination of the linear coefficients A and B was made by defining the correct relative energy at volume expansion 3.0. The Octol EOS's as a function of HMX/TNT content and porosity are given in Table 2. The JWL parameters for the reference 78/22 Octol EOS are given in the top line of this table.

5.0 SHAPED CHARGE JETTING ANALYSIS

The effects of density gradients in the shaped charge explosive were evaluated using a coupled two dimensional hydrodynamic FE/PER theory shaped charge jetting analysis approach [5]. The charge geometry used in the analysis was the BRL 81 mm precision charge [6]. A finite element mesh of the charge is shown in Figure 7. The left hand side of the figure shows an outline of the charge geometry with six layers of explosive. The right hand side shows the finite element mesh. A beta burn model [7] was used to simulate the detonation wave propagation through the multiple layers of explosive.

In the three calculations that were run using the mesh shown in Figure 7, the only variable changed was the explosive equation of state. A summary of the HE materials for each layer is given in the right hand side of the figure. The first calculation used the standard 78/22 Octol JWL equation of state throughout the charge. The jet configuration from this analysis was used as a reference for comparison to analyses with an axial gradient and a circumferential gradient in the charge.

The axial gradient analysis was run with an HMX/TNT gradient from 60/40 at the initiation point to 85/15 at the base of the liner. The gradient in the liner region was from 70/30 to 85/15. One percent porosity was assumed for all explosives in the charge. Comparison to the reference analysis was made by plotting the ratio of the jet velocity of the calculations as a function of liner axial coordinate as shown in Figure 8. This curve is a plot of the reference jet velocity (78/22 Octol) divided by the gradient HE (60/40 to 85/15) jet velocity. This curve shows that the 78/22 Octol gives a slightly higher tip velocity while the gradient charge gives a slightly higher tail velocity.

HMX	TNT	AIR	RHO	PCJ	VEL	E0	GAM	A	B	R1	R2	W
78	22	1.2	1.821	0.342	0.848	0.096	2.830	7.4860	0.1338	4.50	1.20	0.38
60	40	0	1.796	0.314	0.819	0.0876	2.830	6.8725	0.1236	4.50	1.20	0.38
62	38	0	1.801	0.318	0.822	0.0888	2.829	6.9558	0.1255	4.50	1.20	0.38
64	36	0	1.806	0.322	0.826	0.0899	2.829	7.0408	0.1273	4.50	1.20	0.38
66	34	0	1.812	0.326	0.830	0.0910	2.828	7.1274	0.1291	4.50	1.20	0.38
68	32	0	1.817	0.330	0.834	0.0921	2.828	7.2160	0.1308	4.50	1.20	0.38
70	30	0	1.822	0.335	0.838	0.0933	2.828	7.3069	0.1325	4.50	1.20	0.38
72	28	0	1.827	0.339	0.842	0.0944	2.828	7.3995	0.1340	4.50	1.20	0.38
74	26	0	1.833	0.343	0.846	0.0956	2.829	7.4940	0.1355	4.50	1.20	0.38
76	24	0	1.838	0.347	0.850	0.0967	2.830	7.5911	0.1368	4.50	1.20	0.38
78	22	0	1.844	0.351	0.854	0.0979	2.831	7.6903	0.1380	4.50	1.20	0.38
80	20	0	1.849	0.356	0.859	0.0991	2.833	7.7918	0.1392	4.50	1.20	0.38
82	18	0	1.854	0.360	0.863	0.1003	2.835	7.8957	0.1402	4.50	1.20	0.38
84	16	0	1.860	0.364	0.867	0.1015	2.837	8.0024	0.1411	4.50	1.20	0.38
85	15	0	1.863	0.366	0.869	0.1021	2.838	8.0562	0.1416	4.50	1.20	0.38
60	40	1	1.778	0.307	0.813	0.0862	2.831	6.7179	0.1198	4.50	1.20	0.38
62	38	1	1.783	0.311	0.817	0.0873	2.830	6.7989	0.1217	4.50	1.20	0.38
64	36	1	1.788	0.315	0.821	0.0884	2.829	6.8812	0.1236	4.50	1.20	0.38
66	34	1	1.794	0.318	0.824	0.0893	2.833	6.9681	0.1233	4.50	1.20	0.38
68	32	1	1.799	0.323	0.829	0.0906	2.827	7.0515	0.1272	4.50	1.20	0.38
70	30	1	1.804	0.327	0.833	0.0918	2.827	7.1395	0.1289	4.50	1.20	0.38
72	28	1	1.809	0.331	0.837	0.0929	2.827	7.2290	0.1305	4.50	1.20	0.38
74	26	1	1.814	0.335	0.841	0.0940	2.828	7.3210	0.1320	4.50	1.20	0.38
76	24	1	1.820	0.340	0.845	0.0952	2.828	7.4144	0.1335	4.50	1.20	0.38
78	22	1	1.825	0.344	0.849	0.0963	2.829	7.5109	0.1347	4.50	1.20	0.38
80	20	1	1.830	0.349	0.854	0.0977	2.825	7.6066	0.1383	4.50	1.20	0.38
82	18	1	1.836	0.352	0.857	0.0987	2.832	7.7088	0.1372	4.50	1.20	0.38
84	16	1	1.841	0.356	0.861	0.0999	2.834	7.8116	0.1382	4.50	1.20	0.38
85	15	1	1.844	0.359	0.863	0.1005	2.835	7.8638	0.1387	4.50	1.20	0.38
60	40	2	1.760	0.300	0.808	0.0848	2.831	6.5637	0.1162	4.50	1.20	0.38
62	38	2	1.765	0.304	0.812	0.0859	2.829	6.6427	0.1182	4.50	1.20	0.38
64	36	2	1.770	0.308	0.816	0.0870	2.828	6.7230	0.1201	4.50	1.20	0.38
66	34	2	1.775	0.312	0.820	0.0881	2.827	6.8049	0.1219	4.50	1.20	0.38
68	32	2	1.781	0.316	0.824	0.0892	2.827	6.8885	0.1237	4.50	1.20	0.38
70	30	2	1.786	0.320	0.828	0.0903	2.826	6.9736	0.1254	4.50	1.20	0.38
72	28	2	1.791	0.324	0.832	0.0914	2.826	7.0606	0.1271	4.50	1.20	0.38
74	26	2	1.796	0.328	0.836	0.0925	2.826	7.1496	0.1287	4.50	1.20	0.38
76	24	2	1.801	0.332	0.840	0.0937	2.827	7.2404	0.1302	4.50	1.20	0.38
78	22	2	1.807	0.336	0.844	0.0948	2.827	7.3329	0.1316	4.50	1.20	0.38
80	20	2	1.812	0.340	0.848	0.0959	2.828	7.4280	0.1329	4.50	1.20	0.38
82	18	2	1.817	0.344	0.852	0.0971	2.830	7.5260	0.1340	4.50	1.20	0.38
84	16	2	1.823	0.349	0.856	0.0983	2.831	7.6242	0.1353	4.50	1.20	0.38
85	15	2	1.825	0.351	0.858	0.0989	2.832	7.6744	0.1359	4.50	1.20	0.38

Table 2. JWL EOS for Octol as a function of HMX/TNT content and porosity.

The total range of the change in jet velocity is about 5% , which is smaller than one might expect from such a large variation in explosive composition. It is also interesting that the gradient HE charge produces a jet that is probably shorter because of the lower tip velocity and higher tail velocity.

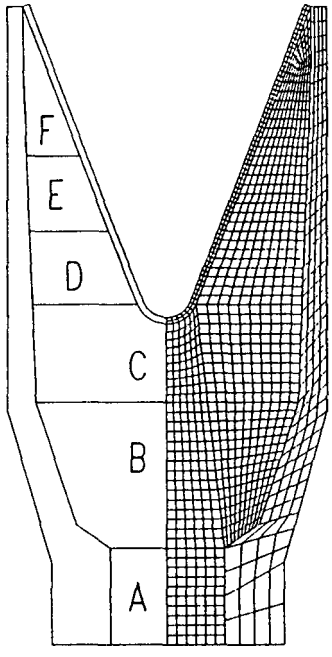

Region	Reference Analysis	Axial Gradient	Circum. Gradient
A	78/22	60/40	78/22
	1.821	1.778	1.821
B	78/22	66/34	78/22
	1.821	1.794	1.821
C	78/22	70/30	78/22
	1.821	1.804	1.821
D	78/22	76/24	78/22
	1.821	1.820	1.821
E	78/22	80/20	82/18
	1.821	1.830	1.836
F	78/22	85/15	78/22
	1.821	1.844	1.821

Figure 7. Finite Element Mesh of BRL 81mm Precision Charge.

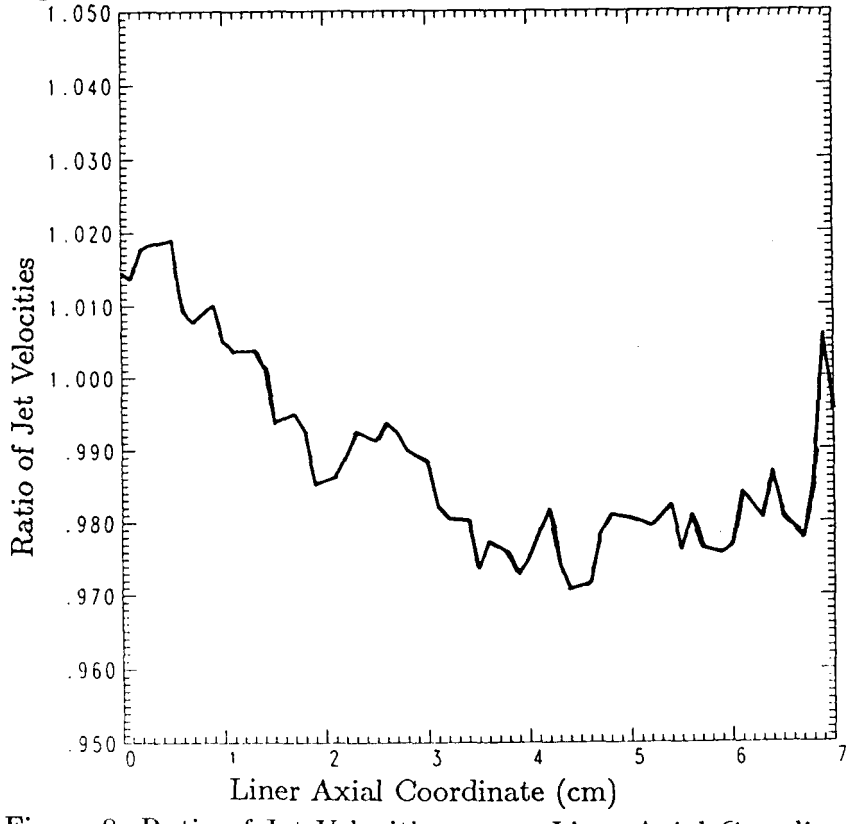

Figure 8. Ratio of Jet Velocities versus Liner Axial Coordinate.

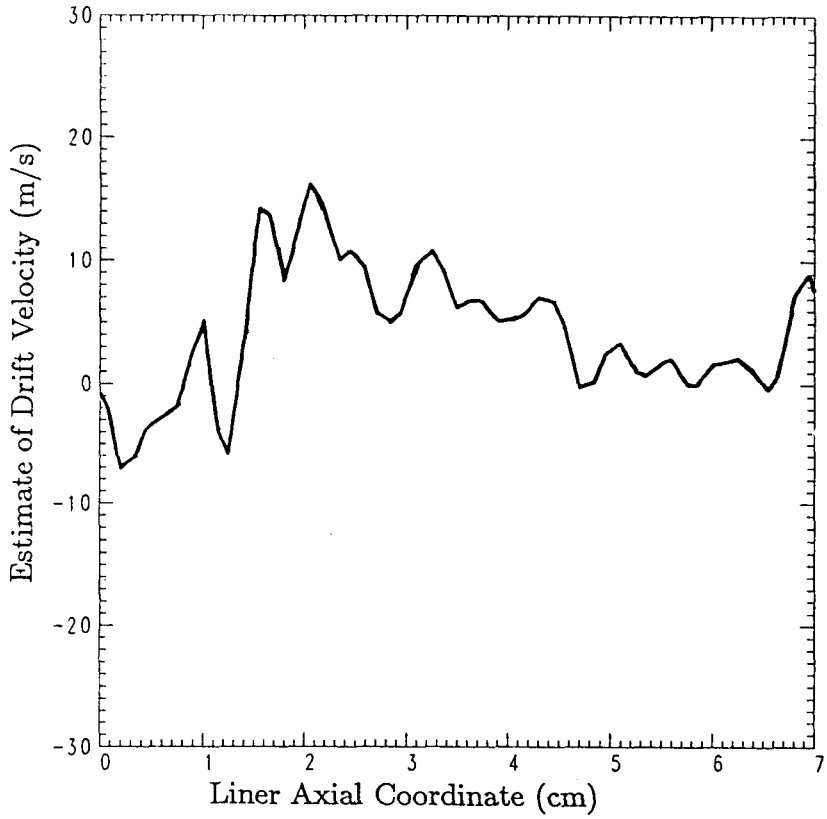

Figure 9. Estimate of Jet Drift Velocity versus Liner Axial Coordinate.

The circumferential gradient analysis was an attempt to determine the magnitude of the lateral drift velocity of the jet that would result from a circumferential gradient in HE composition at a specific elevation in the charge. For this calculation, the reference 78/22 Octol was used everywhere except in region E where it was replaced with 82/18 Octol. An estimate of the resulting jet drift velocity was made by assuming that the 78/22 reference analysis represents the opposite side of the charge without a HE gradient. The drift velocity estimate was made by assuming conservation of radial momentum at the time of liner collapse. Since the liner mass is the same for both calculations, the drift velocity is assumed to be half of the difference in the radial component of the collapse velocity of the two analyses. This estimate of peak drift velocity is plotted in m/s as a function of liner axial coordinate in Figure 9. The magnitude of the drift velocities calculated are consistent with those that have been measured by Segletes for Octol loaded charges [8].

6.0 CONCLUSIONS

An approach for estimating the effects of both axial and circumferential density gradients in a shaped charge explosive load has been studied. The effect of an axial HMX/TNT composition gradient of 60/40 to 85/15 was small when compared to a constant 78/22 HMX/TNT charge load. It was also shown that a charge with such a gradient would produce a shorter jet due to the lower tip velocity and higher jet tail velocity. A circumferential gradient of 78/22 to 82/18 HMX/TNT in one region of the explosive produced a peak drift velocity of about 20 m/s. Although small, a 20 m/s drift

velocity will have definite detrimental effects on performance of the charge at optimum standoff distances.

These calculations show that the reduction of gradients in the explosive load of a charge will produce the best jet characteristics. A sedimentation melt cast loading approach that produces a "HMX rich" explosive in the liner region also opens up the possibility of circumferential gradients. There appears to be no increase in performance from the axial gradient studied, while the potential decrease in performance due to drift velocity from a circumferential gradient is very likely.

7.0 REFERENCES

1. W. F. Larsen, "HMX Distribution and Octol Density Variation in Shaped Charge Warheads," Picatinny Arsenal, TM-2134, April 1974.

2. B. M. Dobrats and P. C. Crawford, "Properties of Chemical Explosives and Explosive Simulants," Lawrence Livermore National Laboratory, UCRL-52997 Change 2, 1985.

3. M. Cowperthwaite and W. H. Zwisler, "TIGER Computer Code Documentation," Stanford Research Institute, May 1975.

4. E. L. Lee, H. C. Hornig, and J. W. Kury, "Adiabatic Expansion of High Explosive Detonation Products," Lawrence Livermore National Laboratory, UCRL-50422 (1968).

5. M. J. Murphy, "Users Guide for 2DJET Analysis of Shaped Charges," Lawrence Livermore National Laboratory, UCID-21415, July 1988.

6. J. Simon and R. DiPersio, "Jet Formation and Utilization," Presented at the Twelth Annual Symposium, Behavior and Utilization in Engineering Design, New Mexico, March 1972.

7. J. P. Woodruff, "KOVEC User's Manual," Lawrence Livermore National Laboratory, UCID-17306 (1976).

8. S. B. Segletes, "Improved Drift Velocity Computations for Shaped Charge Jets," US ARMY Ballistic Research Laboratory, BRL-TR-2823, June 1987.